

A Modeling Method of the Cable Driven Parallel Manipulator for FAST

Rui Yao, Hui Li and Xinyu Zhang

Abstract A Five Hundred meter Aperture Spherical radio Telescope (FAST) is being built in China, and a similarity model was set up in Beijing for further study of FAST. In FAST, A six-cable driven parallel manipulator is adopted as the first level adjustable feed support system. This paper addresses the complete modeling method of the six-cable driven parallel manipulator of FAST with cable mass and elastic deformation. Comparing with the precise catenary modeling equation, modeling and solution of line equation is easier and quicker, but has modeling error for cable driven parallel manipulator. Hence, analysis and compensation method of the modeling error is studied in detail, which encourages the line equation to model and solve the six-cable driven parallel manipulator accurately. Finally, simulation and experiment have been done for supporting the modeling and error compensation methods in this paper.

1 Introduction

China is building a Five-hundred meter Aperture Spherical radio Telescope (FAST) [1]. Figure 1 shows the conceptualization of the FAST system, where the feed support system moves over the active reflector. The feed support system of FAST includes two parts: first-level adjustable feed support system, which is a six-cable driven parallel manipulator with large span that provides the coarse positioning, and a second-level adjustable feed support system (A–B rotator and a Stewart platform) that can compensate the positioning error and achieve the required accuracy. At present, a

R. Yao (✉) · H. Li · X. Zhang
National Astronomical Observatories, Chinese Academy of Sciences, Beijing 100012, China
e-mail: ryao@nao.cas.cn, lihui@nao.cas.cn

X. Zhang
Graduate University of Chinese Academy of Sciences, Beijing 100049, China
e-mail: xyzhang@nao.cas.cn

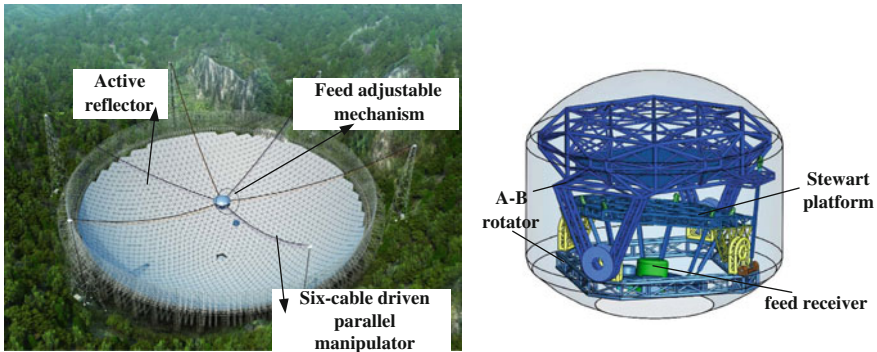


Fig. 1 Conceptual model of the FAST

similarity model of the feed support system is set up in Beijing [2]. Cable driven parallel manipulator has advantages of simple configuration, high load ability, large workspace, low price and high speed [3, 4].

For modeling cable driven parallel manipulators with large span, previous researches did plenty of work on it [5–7]. In order to get highly modeling accuracy, precise catenary equation is adopted. Comparing with the precise catenary equation, modeling and solution of simplified catenary equations are easier and quicker, which are more suitable for real-time calculation and control of cable driven parallel manipulator with large span. However, simplified catenary equations will lead to modeling error, which may not be accepted in real control [5]. So the modeling error should be analyzed and compensated in real application. This paper is expected to fill that gap.

In this paper, complete modeling equations with cable mass and elastic deformation based on the precise catenary and simplified catenary equations will be set up for the six-cable driven parallel manipulator in Sect. 2. Then, a modeling compensation method will be discussed in Sect. 3 to enhance the modeling accuracy of the simplified modeling method for the six-cable driven parallel manipulator. From experiment, the simplified modeling method with a compensation equation can satisfy control accuracy of the six-cable driven parallel manipulator.

2 Modeling of the Six-Cable Driven Parallel Manipulator with Large Span

For building the FAST, a six-cable driven parallel manipulator is adopted as the first-level adjustable feed support system, and a similarity model of the six-cable driven parallel manipulator is set up in Beijing. This section will discuss the modeling method of the six-cable driven parallel manipulator. Considering cable mass and

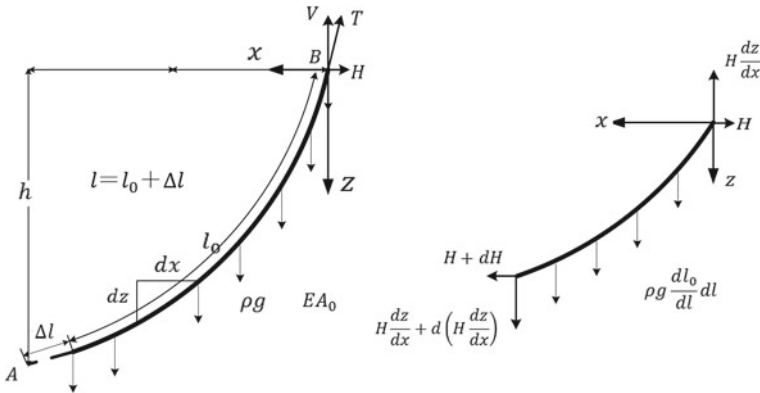


Fig. 2 Precise catenary modeling of a cable

elastic deformation, precise catenary equation and simplified catenary equations are set up in this section.

2.1 Modeling Equations of Single Cables

2.1.1 Precise Catenary Equation

For setting up a cable model with precise catenary equation, the symbols used in Fig. 2 are defined as: l_0 is the unstrained length of the cables; Δl the strain of the cable; T the tension applied to the fixed end of the cable; ρ the unstrained linear density; E the elastic modulus; A_0 the unstrained cross-sectional area; H the horizontal component of the cable tension vector and V its vertical component. Using the variables and coordinate system above, we will briefly reproduce Irvines derivation [8] in this paper.

As shown in Fig. 2 a point along the length of the strained cable can be denoted by Cartesian coordinate and. To begin with, the cable must satisfy the geometric constraint:

$$\sum x = 0 \quad H + dH - H = 0 \tag{1}$$

$$\sum z = 0 \quad H \frac{dz}{dx} + d\left(H \frac{dz}{dx}\right) + \rho g dl_0 - H \frac{dz}{dx} = 0 \tag{2}$$

where,

$$\frac{dl}{dl_0} = \frac{T}{EA_0} + 1 \tag{3}$$

$$T = H\sqrt{1 + \left(\frac{dz}{dx}\right)^2} \tag{4}$$

From $dl = dx\sqrt{1 + \left(\frac{dz}{dx}\right)^2}$, Eq. 2 can be expressed as:

$$d\left(H\frac{dz}{dx}\right) + \rho g \frac{EA_0}{T + EA_0} dl = 0 \tag{5}$$

Assuming $\frac{dz}{dx} = p$, Eq. 5 can be written as:

$$\frac{dp}{dx} + \frac{\rho g EA_0}{H} \frac{\sqrt{1 + p^2}}{H\sqrt{1 + p^2} + EA_0} = 0 \tag{6}$$

Therefore,

$$x = -\frac{H}{\rho g} sh^{-1}\left(\frac{dz}{dx}\right) - \frac{H^2}{\rho g EA_0} \frac{dz}{dx} + c \tag{7}$$

Where,

$$sh^{-1}(x) = \ln\left(x + \sqrt{1 + x^2}\right), x \in (-\infty, +\infty) \tag{8}$$

$$x = -\frac{H}{\rho g} \ln\left(\frac{dz}{dx} + \sqrt{1 + \left(\frac{dz}{dx}\right)^2}\right) - \frac{H^2}{\rho g EA_0} \frac{dz}{dx} + c \tag{9}$$

Integrating and applying the boundary conditions as follows:

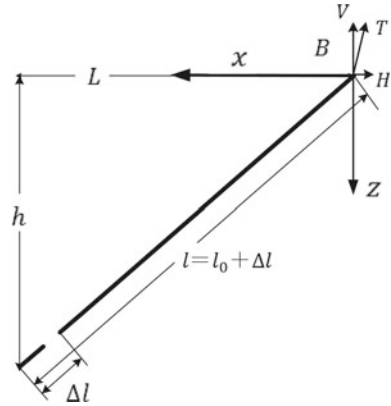
$$\begin{aligned} x = 0, z = 0 \\ x = L, z = h \end{aligned} \tag{10}$$

The length of cable is l , the unstrained length of the cable is l_0 , and Δl represents the strain of the cable. The relationship can be expressed as: $l = l_0 + \Delta l$.

$$l = \int_0^l \sqrt{1 + \left(\frac{dz}{dx}\right)^2} dx \tag{11}$$

$$l_0 = \int \frac{1}{\frac{T}{EA_0} + 1} dl \tag{12}$$

Fig. 3 Line modeling of a cable



2.1.2 Line Equation

A line is shown in Fig. 3. A cable under its mass cannot remain straight. The idealization would be possible if the ends of the cable were subjected to tensions that are predominantly larger than the effect of the cable mass or the accuracy requirement is not high.

In Fig. 3, line equation with elastic deformation of a cable can be easily derived as follows:

$$l = (h^2 + L^2)^{1/2} \tag{13}$$

$$T = (V^2 + H^2)^{1/2} \tag{14}$$

$$L = l \frac{H}{T} \tag{15}$$

$$h = l \frac{V}{T} \tag{16}$$

$$\Delta l = \frac{Tl}{EA_0} \tag{17}$$

where Δl is elastic deformation of the cable.

2.2 Modeling of the Six-Cable Driven Parallel Manipulator

In Fig. 4, for studying the largest radio telescope FAST, a similarity model of FAST is set up in Beijing. The related geometric parameters of the six-cable driven parallel manipulator in the similarity model are given in Table 1 [9].



Fig. 4 40m diameter six-cable driven parallel manipulator

Table 1 Geometric parameters of the six-cable driven parallel manipulator

Symbol	Quantity	Value
r_a	Radius of the moving platform	0.5 (m)
r_b	Radius of cable towers distributed circle	20 (m)
h	Height of cable tower	18 (m)
d	Diameter of cable	8 (mm)
ρ	Density of cable	0.5145 (kg/m)
m_o	Mass of moving platform	213 (kg)
E	Youngs modular	1.6×10^{11} (Pa)

In Fig. 5, two coordinates are set up for the six-cable driven parallel manipulator: an inertial frame $\mathfrak{N} : O - XYZ$ is located at the center of the reflectors bottom. Another moving frame $\mathfrak{N}' : O' - X'Y'Z'$ is located at the center of the moving platform. B_i ($i = 1, 2, \dots, 6$) are the connected points of the cables and cable towers, and A_j ($j = 1, 2, 3$) are the connected points of the cables and moving platform.

For analyses, the symbols used in this section are defined as: $O'\mathfrak{N}$ is the O' expressed in the inertial frame; $B_i^{\mathfrak{N}}$ the vector B_i expressed in the inertial frame; $A_j^{\mathfrak{N}}$ the vector A_j expressed in the inertial frame; $A_j^{\mathfrak{N}'}$ the vector A_j expressed in the moving frame; r_b the radius of the cable towers distributed circle; r_a the radius of the moving platform; h the height of the cable tower.

According to Fig. 5, the vector of the cables can be expressed as:

$$B_i^{\mathfrak{N}} = [r_b \cos((i - 1)\pi/3), r_b \sin((i - 1)\pi/3), h]^T, \quad i = 1, 2, \dots, 6 \quad (18)$$

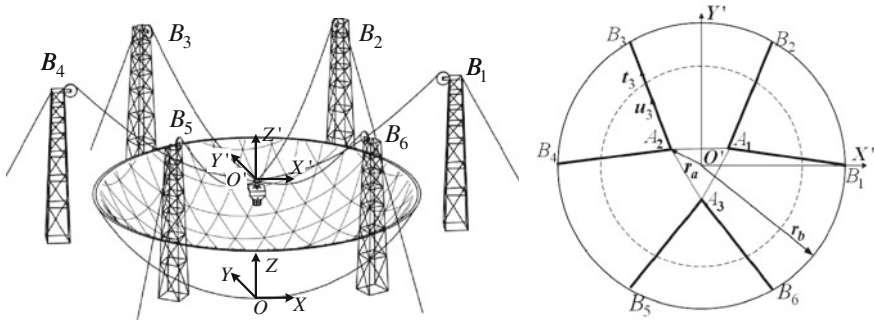


Fig. 5 Geometric parameter of the six-cable driven parallel manipulator

$$A_j^{3l'} = [r_a \cos((4j - 3)\pi/6), r_a \sin((4j - 3)\pi/6), 0]^T, \quad j = 1, 2, 3 \quad (19)$$

$$A_j^{3l} = R \cdot A_j^{3l'} - O'^{3l} \quad (20)$$

where R is the coordinate-axis rotation matrix.

Assuming $L_i = A_j^{3l} - B_i^{3l}$, $u_i = L_i / \|L_i\|$, $r_i = A_j^{3l} - O'^{3l}$, static equilibrium equation of the six-cable driven parallel manipulator can be written as:

$$F = J^T \sigma \quad (21)$$

where σ is the cable tension vector; J^T the tension transmission matrix of the cable driven parallel manipulator; $F \in R^n$ the wrench of the moving platform.

$$\sigma = [\sigma_1, \sigma_2, \dots, \sigma_6]^T \quad (22)$$

$$J^T = \begin{pmatrix} u_1 & \cdots & u_6 \\ r_1 \times u_1 & \cdots & r_6 \times u_6 \end{pmatrix} \quad (23)$$

According to Eqs. 21–23, initial cable length and cable tension of the six-cable driven parallel manipulator can be calculated. Putting the initial cable tension into the two single cable modeling equations, the real cable length and tension can be calculated by using iterative algorithm. The cable tensions of the six-cable driven parallel manipulator should satisfy:

$$\begin{aligned} \sum_{i=1}^6 \sigma_{ix} &= 0, \quad \sum_{i=1}^6 \sigma_{iy} = 0, \quad \sum_{i=1}^6 \sigma_{iz} = 0 \\ \sum_{i=1}^6 M_{ix} &= 0, \quad \sum_{i=1}^6 M_{iy} = 0, \quad \sum_{i=1}^6 M_{iz} = 0 \end{aligned} \quad (24)$$

where $\sum_{i=1}^6 \sigma_{ix}$ is the tension in X-direction of the six-cable driven parallel manipulator, and $\sum_{i=1}^6 M_{ix}$ is the torque in X-direction of the six-cable driven parallel manipulator.

3 Modeling Error Analysis and Compensation of the Six-Cable Driven Parallel Manipulator

3.1 Modeling Error Analysis

When the terminal pose of the moving platform is at $\mathbf{O}' = [x, y, z, \alpha, \beta, \gamma]^T$, the inverse kinematics equation for the six-cable driven parallel manipulator can be written as:

$$\mathbf{l} = \Gamma (\mathbf{O}') \tag{25}$$

where $\mathbf{l} = (l_1, l_2, \dots, l_i)$ ($i = 1, 2, \dots, 6$) represents the cable length.

Therefore, the inverse solutions of the six-cable driven parallel manipulator by line modeling equation can be written as:

$$l_i = \Gamma_l (\mathbf{O}') \tag{26}$$

where l_i are the length of the cable arc calculated by the line modeling equation.

The solutions of the six-cable driven parallel manipulator based on precise catenary can be expressed as:

$$\Theta (\mathbf{l}) = \mathbf{O}' \tag{27}$$

So, the modeling error vector of the six-cable driven parallel manipulator by line modeling equation is:

$$\varepsilon_l = \Theta (\mathbf{l}_l) - \mathbf{O}' \tag{28}$$

where $\varepsilon_l = [\varepsilon x_l, \varepsilon y_l, \varepsilon z_l, \varepsilon \alpha_l, \varepsilon \beta_l, \varepsilon \gamma_l]^T$ are the error vectors of the six-cable driven parallel manipulator caused by line modeling equation.

For meeting the modeling accuracy requirement of the six-cable driven parallel manipulator, the error compensation target can be expressed as:

$$\min \left(\sqrt{\frac{\sum_1^k (\varepsilon x_{line}^2 + \varepsilon y_{line}^2 + \varepsilon z_{line}^2)}{k}} \right), \quad k = 1, 2, \dots \tag{29}$$

The compensation conditions are:

$$\sqrt{\varepsilon x_{line}^2 + \varepsilon y_{line}^2 + \varepsilon z_{line}^2} \leq \varepsilon_0 \tag{30}$$

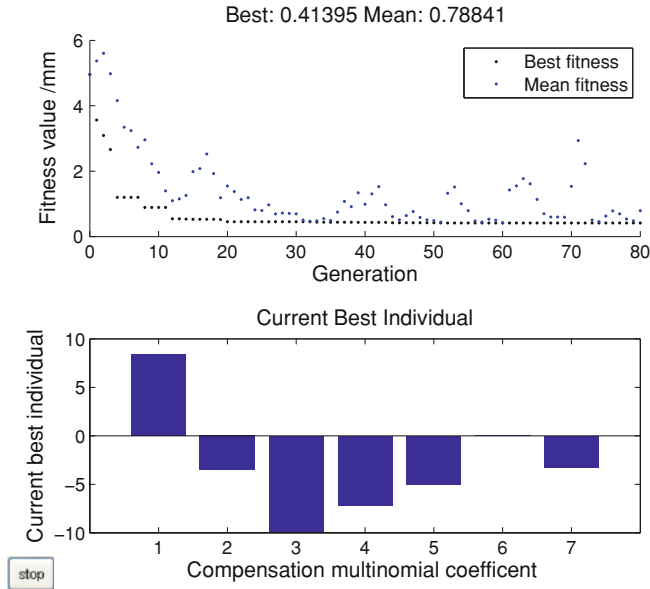


Fig. 6 Compensation polynomial coefficients of line equation

where

$$\varepsilon_{line} = \Theta (l_l + \varepsilon l_l) - \mathbf{O}' \tag{31}$$

$$l_l = \Gamma_l (\mathbf{O}') \tag{32}$$

$$\varepsilon_{line} = (\varepsilon x_{line}, \varepsilon y_{line}, \varepsilon z_{line}, \varepsilon \alpha_{line}, \varepsilon \beta_{line}, \varepsilon \gamma_{line})^T \tag{33}$$

The kinematic control accuracy of the six-cable driven parallel manipulator is Root Mean Square 10 mm (RMS 10mm). The maximum allowed modeling error ε_0 is given as 1 mm. For meeting the modeling accuracy requirement, a modeling error compensation polynomial is introduced as Eq. 34.

$$\begin{aligned} \varepsilon l_l = f(L, H, h) = & \left(a_1 \times L^2 - a_2 \times L - b_1 \times h^2 - b_2 \times h \right) \times 10^{-6} \\ & + \left(-c_1 \times 10^{-4} \times H^2 + c_2 \times 10^{-2} \times H - d \right) \times 10^{-6} \end{aligned} \tag{34}$$

The compensation polynomial coefficients for the line equation can be optimized by genetic algorithm in Fig. 6. From Fig. 6, we obtain the expected error result of this modeling is about RMS 0.78841mm.

Therefore, the compensation polynomial for the line equation is:

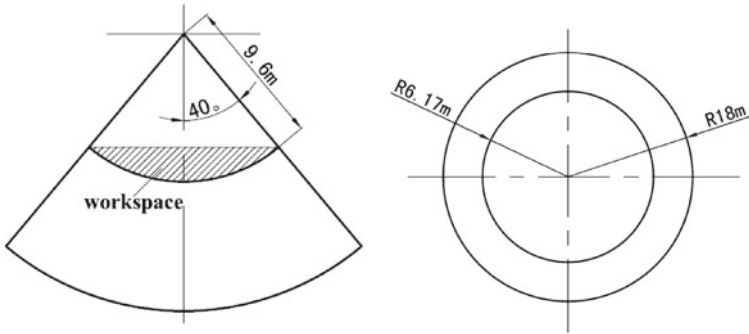


Fig. 7 Required workspace of the six-cable driven parallel manipulator

Fig. 8 Experimental trajectories-line

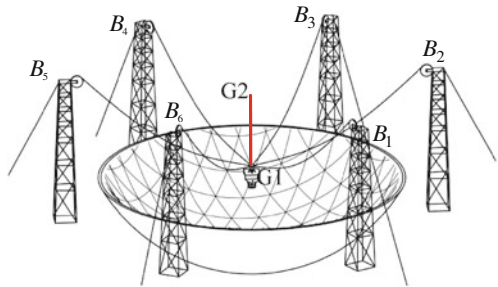
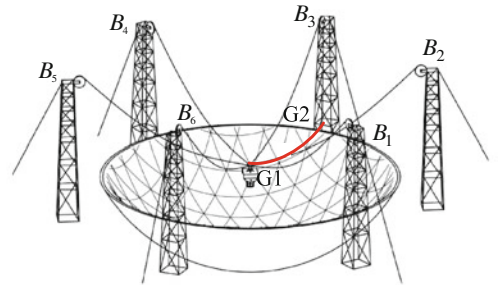


Fig. 9 Experimental trajectories-arc



$$\begin{aligned} \varepsilon_{l1} = & \left(8.3721 \times L^2 - 3.5328 \times L - 9.8747 \times h^2 - 7.1498 \times h \right) \times 10^{-6} \\ & + \left(-5.0527 \times 10^{-4} \times H^2 + 0.0894 \times 10^{-2} \times H - 3.2483 \right) \times 10^{-6} \end{aligned} \tag{35}$$

Fig. 10 Experimental trajectories-circle

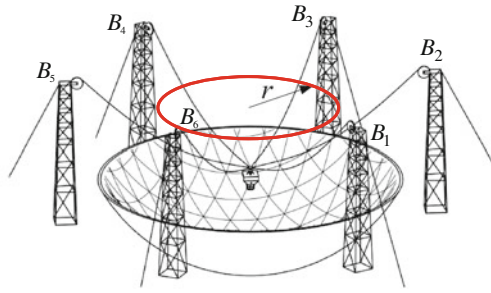


Fig. 11 Total station



3.2 Simulation and Experiment

In Fig. 7, required workspace of the six-cable driven parallel manipulator is presented as a sphere crown surface for studying the modeling error and error compensation methods.

For proving the feasibility of the error compensation method of the six-cable driven parallel manipulator, three experimental trajectories are introduced in Figs. 8, 9, 10. The three experimental trajectories are line, arc and circle respectively.

In Fig. 8, the line trajectory is from $G_1 = (0, 0, 8.4\text{ m})$ to $G_2 = (0, 0, 9.4\text{ m})$, and the kinematic velocity is $v = 2.3\text{ mm/s}$.

In Fig. 9, the arc trajectory is from $G_1 = (0, 0, 8.4\text{ m})$ to $G_2 = (2, 0, 8.7\text{ m})$ with pose angle from 0° to 6° , and the kinematic velocity is $v = 2.5\text{ mm/s}$.

Fig. 12 Kinematic control accuracy of line trajectory

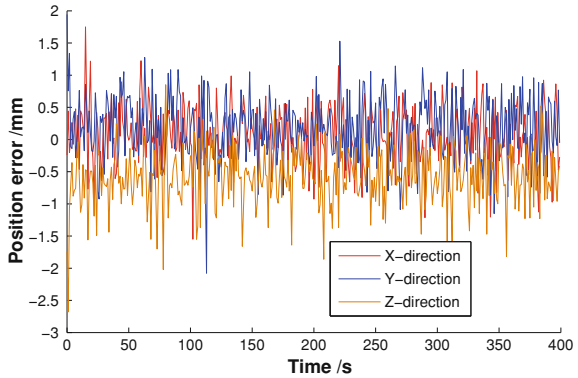


Fig. 13 Kinematic control accuracy of arc trajectory

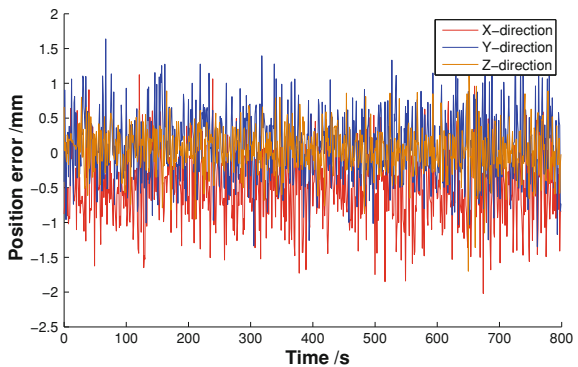


Figure 10 shows that the center of circle trajectory is at (0, 0, 8.7 m), and the radius of the circle trajectory is $r = 2$ m with 6° pose angle. The kinematic velocity of the circle trajectory is $v = 6.3$ mm/s .

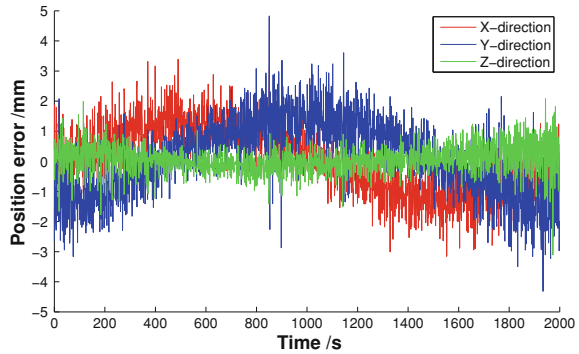
Without kinematic control of the second feed support system, the kinematic control accuracy of the six-cable driven parallel manipulator can be measured by Total Station which is shown in Fig. 11.

The kinematic control errors of the six-cable driven parallel manipulator on the three experimental trajectories are shown in Figs. 12, 13, 14.

From Figs. 12, 13, 14, we know that the kinematic control accuracies of the six-cable driven parallel manipulator on line, arc and circle trajectories are RMS 1.001 mm, RMS 0.929 mm and RMS 1.703 mm respectively.

According to the kinematic control experiment, the accuracy of the six-cable driven parallel manipulator can meet the requirement, which proves the simplified modeling and compensation method in this paper are feasible and accurate.

Fig. 14 Kinematic control accuracy of circle trajectory



4 Conclusions

This paper addressed the modeling method of a six-cable driven parallel manipulator with large span in FAST. Considering the cable mass and elastic deformation, completely modeling equations are derived in detail based on precise and simplified catenary equations. The modeling error of the six-cable driven parallel manipulator caused by simplified catenary equations is analyzed, and a modeling error compensation method is studied. Taking the similarity model as example, error compensation polynomial coefficients are optimized by genetic algorithm. Finally, the experiment result indicates that the modeling and error compensation method in this paper can satisfy kinematic accuracy.

Acknowledgments This paper is supported by the National Natural Science Foundation under Grant No. 10973023 and 11103046.

References

1. Nan, R.D.: Five hundred meter aperture spherical radio telescope (FAST). *Sci. China Ser. G Phys. Mech. Astron.* **49**(2), 129–148 (2006).
2. Yao, R., Tang, X.Q., Wang, J.S.: Cable tension analysis and optimization of radio telescope feed support system (in Chinese). *Prog. Nat. Sci.* **19**(11), 1211–1229 (2009)
3. Fang, S., Frantiza, D., Torlo, M., et al.: Motion control of a tendon-based parallel manipulator using optimal tension distribution. *IEEE/ASME Trans. Mechatron.* **9**(9), 561–568 (2004)
4. Hiller, M., Fang, S.Q.: Design, analysis and realization of tendon-based parallel manipulators. *Mech. Mach. Theory* **40**, 429–445 (2005)
5. Qu, L., Tang, X.Q., Yao, R.: Error analysis and compensation of cable driven parallel manipulator for the forty-meter aperture radio telescope (in Chinese). *High technol. lett.* **20**(4), 303–308 (2010)
6. Taghirad, H.D., Nahon, M.A.: Forward kinematics of a macro-micro parallel manipulator, pp. 1–6. *IEEE/ASME International Conference Advanced Intelligent, Mechatronics* (2007)
7. Lambert, C., Nahon, M., Chalmers, D.: Implementation of an aerostat positioning system with cable control. *IEEE/ASME Trans. Mechatron.* **12**(2), 32–40 (2007)

8. Irvine, H.: *Cable Structures*, pp. 16–20 MIT Press, Massachusetts (1981).
9. Nan, R.D.: *Structure for supporting the feedback cabin of the FAST*. Technical Report, National Astronomical Observatories Chinese Academy of Science (2005)